Orbital, tectonic and oceanographic controls on Pliocene climate and atmospheric circulation in Arctic Norway

Sina Panitz[1], Ulrich Salzmann[1], Bjørg Risebrobakken[2], Stijn De Schepper[2], Matthew J. Pound[1], Alan M. Haywood[3], Aisling M. Dolan[3], Daniel J. Lunt[4]

[1]Department of Geography and Environmental Sciences, Faculty of Engineering and Environment, Northumbria University, Newcastle upon Tyne NE1 8ST, UK, ulrich.salzmann@northumbria.ac.uk, matthew.pound@northumbria.ac.uk

[2]Uni Research Climate, Bjerknes Centre for Climate Research, Jahnebakken 5, 5007 Bergen, Norway, bjorg.risebrobakken@uni.no, stijn.deschepper@uni.no

[3]School of Earth and Environment, University of Leeds, Woodhouse Lane, Leeds LS2 9JT, UK, A.M.Haywood@leeds.ac.uk, A.M.Dolan@leeds.ac.uk

[4]School of Geographical Sciences, University of Bristol, University Road, Bristol BS8 1SS, UK, D.J.Lunt@bristol.ac.uk

Corresponding author: Sina Panitz (E-mail: sina.panitz@gmail.com)

Abstract

During the Pliocene Epoch, a stronger-than-present overturning circulation has been invoked to explain the enhanced warming in the Nordic Seas region in comparison to low to mid-latitude regions. While marine records are indicative of changes in the northward heat transport via the North Atlantic Current (NAC) during the Pliocene, the long-term terrestrial climate evolution and its driving mechanisms are poorly understood. We present the first two-million-year-long Pliocene pollen record for the Nordic Seas region from Ocean Drilling Program (ODP) Hole 642B, reflecting vegetation and climate in Arctic Norway, to assess the influence of oceanographic and atmospheric controls on Pliocene climate evolution. The vegetation record reveals a long-term cooling trend in northern Norway, which might be linked to a general decline in atmospheric CO_2 concentrations over the studied interval, and climate oscillations primarily controlled by precession (23 kyr), obliquity (54 kyr) and eccentricity (100 kyr) forcing. In addition, the record identifies four major shifts in Pliocene vegetation and climate mainly controlled by changes in northward heat transport via the NAC. Cool temperate (warmer than present) conditions prevailed between 5.03–4.30 Ma, 3.90–3.47 Ma and 3.29–3.16 Ma and boreal (similar to present) conditions predominated between 4.30–3.90 Ma, 3.47–3.29 and after 3.16 Ma. A distinct decline in sediment and pollen accumulation rates at c. 4.65 Ma is probably linked to changes in ocean currents, marine productivity and atmospheric circulation. Climate model simulations suggest that changes in the strength of the Atlantic Meridional Overturning Circulation during the Early Pliocene could have affected atmospheric circulation in the Nordic Seas region, which would have affected the direction of pollen transport from Scandinavia to ODP Hole 642B.

Keywords: pollen, vegetation, Pliocene, North Atlantic Current, Central American Seaway

1. Introduction

During the Pliocene Epoch (5.33–2.59 Ma), global mean annual temperatures were 2–3ºC warmer than present (Haywood et al., 2013). Due to positive feedback mechanisms in the Arctic, warming was particularly pronounced at high latitudes (Dowsett et al., 2013). On the land masses surrounding the Nordic Seas, cool temperate and boreal forests reached further north during the Pliocene into regions that are presently covered by subarctic boreal forests and Arctic tundra (Bennike et al., 2002; Panitz et al., 2016; Verhoeven et al., 2013; Willard, 1994). The enhanced warming in the Nordic Seas region has been ascribed to a stronger than present Atlantic Meridional Overturning Circulation (AMOC) and thus North Atlantic

Current (NAC) (Haug et al., 2001; Raymo et al., 1996, 1992). However, an increase in the strength of the AMOC during the Pliocene is not simulated by all climate models (Zhang et al., 2013). In both marine and terrestrial climate model simulations for the Pliocene, temperatures are underestimated at high latitudes and remain below temperatures based on data reconstructions (Dowsett et al., 2013; Salzmann et al., 2013). Palaeogeographic differences have been suggested to account for the data-model mismatch. Simulations with an altered palaeogeography (North Atlantic and Baltic river input, lowered Greenland-Scotland Ridge and exposed Barents Sea) show a strong high latitude warming and weaker AMOC (Hill, 2015). Closing the Bering Strait and the Canadian Arctic Archipelago has been shown to increase warming at high latitudes and to strengthen the AMOC (Otto-Bliesner et al., 2017). Model experiments to assess Pliocene terrestrial temperature change indicate that high insolation, increased CO_2 concentrations and a closed Arctic gateway enhance high-latitude warming (Feng et al., 2017). However, the low resolution and poor age control of most terrestrial records limit the quantification of data-model mismatch at high latitudes (Feng et al., 2017).

Heat is transported to the Arctic Ocean via the Norwegian Atlantic Current (NwAC), the continuation of the NAC in the eastern Nordic Seas. Pliocene marine records of sea surface temperature (SST) and palaeoceanographic changes in the North Atlantic and Nordic Seas indicate repeated variations in the northward heat transport via the NAC (Bachem et al., 2017; De Schepper et al., 2013; Lawrence et al., 2009; Naafs et al., 2010; Risebrobakken et al., 2016). The development of a modern-like surface ocean circulation in the Nordic Seas around 4.5 Ma has been linked to the establishment of a northward flow through the Bering Strait and a shoaling of the Central American Seaway (CAS) (De Schepper et al., 2015). In Ocean Drilling Program (ODP) Hole 642B increased abundances of the dinoflagellate species *Protoceratium reticulatum* after 4.2 Ma suggest increased Atlantic water influence at the site and the establishment of a modern-like NwAC (De Schepper et al., 2015). Alkenone-derived SSTs in Hole 642B show a pronounced cooling at 4.3 Ma, with temperature decreasing by ~5°C to values fluctuating around the Holocene average, which might be linked to a strengthening of the East Greenland Current (EGC) and reduced amplitude of obliquity forcing (Bachem et al., 2017). Carbon isotope changes in Hole 642B are indicative of a well-ventilated Norwegian Sea comparable to the present situation (Risebrobakken et al., 2016). Increasing surface water densities have been inferred at the same site which may be the result of increased Atlantic water influence already from 4.6 Ma (Risebrobakken et al., 2016). Early Pliocene oceanographic changes in the Caribbean indicate that the shoaling of the CAS between 4.8 and 4.0 Ma is associated with a strengthening of the AMOC (Groeneveld et al., 2008; Haug et al., 2001; Osborne et al., 2014; Steph et al., 2010). However, benthic carbon and oxygen isotope records from the Atlantic suggest that deep water circulation remained unaffected by the shoaling of the CAS (Bell et al., 2015). Neogene palaeofloras from North America and Western Eurasia indicate that the difference in the thermal gradients between these two continents developed between the late Miocene and late Pliocene, possibly in response to the intensification of the AMOC after the shoaling of the CAS during the early Pliocene (Utescher et al., 2017). A pronounced warming in the Norwegian Sea took place around 4.0 Ma in response to a strengthened northward heat transport potentially due to the CAS shoaling or a deepening of the Greenland-Scotland Ridge (Bachem et al., 2017). The presence of a warmer NwAC is supported by a corresponding depletion of planktic $\delta^{18}O$ in Hole 642B (Risebrobakken et al., 2016). Contemporaneous cooling in the Iceland Sea resulted in the establishment of a strong zonal gradient and strengthened surface circulation in the Nordic Seas (Bachem et al., 2017; Herbert et al., 2016). The presence of warm surface waters in the Norwegian Sea might have contributed, in addition to regional tectonic uplift, to the development of seasonal sea ice in the Eurasian sector of the Arctic Ocean around 4 Ma

(Knies et al., 2014) by enhancing evaporation and precipitation, and thus Arctic freshwater supply (Bachem et al., 2017).The impact of these palaeoceanographic changes on the terrestrial climate evolution in northern Norway and potential links to the shoaling of the CAS are unknown.

For the Late Pliocene (Piacenzian, 3.60–2.58 Ma), SST reconstructions show a variable pattern in the magnitude of warming, with the largest anomalies being recorded in the Iceland and Greenland Seas (Dowsett et al., 2013; Knies et al., 2014; Schreck et al., 2013) and the lowest in the Norwegian Sea (Bachem et al., 2017, 2016). Decreasing SSTs in the Norwegian Sea between 3.65 and 3.30 Ma are suggested to be the result of a reduced influence of the NAC on the NwAC (Bachem et al., 2017). A new multi-proxy study shows that during the Piacenzian vegetation and climate changes in northern Norway coincide with variations in Atlantic water influence and SST changes in the Norwegian Sea (Panitz et al., 2017). Whereas most Pliocene terrestrial records show warmer-than-present climatic conditions, the reconstruction of terrestrial climate evolution and variability before the onset of extensive Pleistocene Northern Hemisphere Glaciation (NHG) has, however, been hampered by the short temporal coverage of existing records in the Nordic Seas region (Bennike et al., 2002; Verhoeven et al., 2013; Willard, 1994). Here, we investigate the relation between Pliocene oceanographic changes in the North Atlantic and Nordic Seas and terrestrial climate changes in northern Norway over a two-million-year long time period.

This study presents a Pliocene (5.03–3.14 Ma) high-resolution pollen record for the Nordic Seas region, reflecting vegetation changes in northern Norway. The new Early Pliocene pollen record from ODP Hole 642B is combined with the previously published Late Pliocene pollen record from the same site (Panitz et al., 2016) and compared to SST and water mass changes in the Norwegian Sea (Bachem et al., 2017; De Schepper et al., 2015; Risebrobakken et al., 2016). Climate model output is presented to assess potential changes in pollen transport

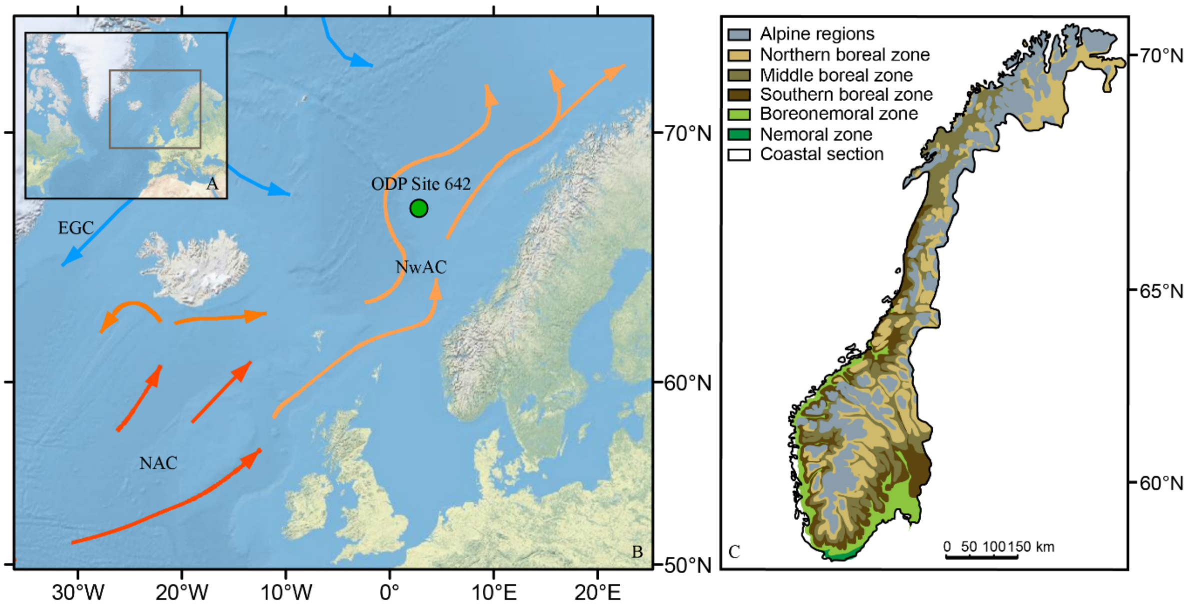

Figure 1: Location of (A) the study area in the North Atlantic and (B) ODP Hole 642B in the Norwegian Sea. (C) Modern vegetation of Norway modified after Moen (1987). In (B), colour coding of currents indicates the relative temperature: dark orange = warm; light orange = moderately warm; blue = cold. EGC = East Greenland Current, NAC = North Atlantic Current and NwAC = Norwegian Atlantic Current.

to the site by wind in response to changes in AMOC strength due to the shoaling of the CAS. The aim of this study is to assess (1) the long-term controls on vegetation and climate changes in northern Norway, (2) the response of vegetation changes to the variability of the NAC, and (3) the potential effects of early Pliocene oceanographic changes on pollen transport to the site.

2. Oceanographic setting and modern vegetation of Norway

ODP Hole 642B was recovered during Leg 104 and is situated about 400–450 km off the coast of Norway on the outer Vøring Plateau in the Norwegian Sea (67°13.2’N, 2°55.8‘E, 1286 m water depth, Shipboard Scientific Party (1987); Figure 1). A branch of the NwAC, which is an extension of the warm NAC, flows northward on either side of the plateau (Orvik and Niiler, 2002). At present, the influence of these warm waters results in relatively mild climatic conditions in Scandinavia (Furevik, 2000). Boreal forest extends over most of

Norway with pure deciduous forests only found along the south coast. The proportion of deciduous and thermophilic elements decreases with increasing latitude, and altitude of the Scandinavian mountains (Moen, 1987). In southern Scandinavia, the altitudinal limit of the tree line is reached at ~1200 m above sea level, with alpine tundra predominating beyond the tree limit (Moen, 1999). The tree line steadily declines with increasing latitude until tundra prevails at sea level in northernmost Norway (Moen, 1999, 1987). Based on the analysis of two (sub)surface samples from Hole 642B, the pollen signal has been shown to be representative of the prevailing vegetation in northern Norway (Panitz et al., 2016). The predominance of wind-pollinated taxa in the (sub)surface and Pliocene samples suggests that pollen is mainly transported to the site by wind. While plumes of cold fjord water enter the Norwegian Sea during spring at present and extend up to 100 km offshore (Mork, 1981), such plumes most likely did not develop during the Pliocene due to the absence of fjords and a reduced ice cover. There is no evidence of the existence of large rivers during the Pliocene, with modest sedimentation along the Norwegian continental margin during the Middle Eocene to Pliocene. Sedimentation rates increased greatly with the onset of NHG around 2.6 Ma (Eidvin et al., 2000; Faleide et al., 2008).

3. Materials and Methods

3.1. Age model

The age model for the Pliocene section of ODP Hole 642B is based on the updated magnetic stratigraphy of Bleil (1989) to the ATNTS2012 time scale (Hilgen et al., 2012) and correlation of the benthic $\delta^{18}O$ curve from Hole 642B to the global LR04 benthic $\delta^{18}O$ stack between 4.147 and 3.14 Ma (Lisiecki and Raymo, 2005; Risebrobakken et al., 2016). A major hiatus exists in the Late Pliocene section of the record after 3.14 Ma (Bleil, 1989; Risebrobakken et al., 2016). The tie points for the age model (Supplementary Table 1) are shown alongside the sedimentation rate in Figure 3 (Risebrobakken et al., 2016), with changes in sedimentation rate reflecting the position of the tie points.

3.2. Sample preparation and pollen analysis

A total of 128 samples were selected for pollen analysis between 83.55 and 66.95 metres below sea floor (mbsf) from ODP Hole 642B, ranging in age from 5.03 to 3.14 Ma (Risebrobakken et al., 2016). The samples were pre-sieved in Bergen, Norway through a 63 µm mesh to retain foraminifera for oxygen isotope analysis (Risebrobakken et al., 2016). A potential bias in the pollen data due to the loss of larger Pinaceae grains has been excluded by comparison of sieved and unsieved samples (Panitz et al., 2016). Sample preparation was carried out at the Palynological Laboratory Services Ltd, North Wales and Northumbria University, Newcastle, using standard palynological techniques (Faegri and Iversen, 1989). In order to calculate pollen concentrations, one *Lycopodium clavatum* spore tablet was added to each sample (Stockmarr, 1971). The treatment with cold HCl (20%) was followed by the use of cold, concentrated HF (48%) to remove carbonates and silicates, respectively. An additional wash with hot (c. 80°C) HCl (20%) was conducted to remove fluorosilicates. After back-sieving the sediment through a 10 µm screen, the residue was mounted on glass slides using glycerol-gelatine jelly. Pollen analysis was carried out using a Leica Microscope (DM 2000 LED) at magnifications of 400x and 1000x. The identification of pollen and spores was aided by the pollen reference collection at Northumbria University and the use of literature (e.g. Beug, 2004). Reworked pollen and spores were differentiated from in situ grains based on the thermal maturity of the exine, with reworked grains having orange to brown colours, and/or their presence outside their stratigraphic range. Particularly reworked gymnosperm pollen showed a high degree of compression, a faint alveolar structure of the saccae and mineral imprints (de Vernal and Mudie, 1989a, 1989b; Willard, 1996). In situ *Lycopodium clavatum* spores differed in colour from the marker spores.

For the majority of samples more than 300 pollen and spore grains were counted. Only 20 samples yielded a total count of less than 300 grains. Percentages of pollen and spores were calculated based on the pollen sum, excluding *Pinus* pollen as well as unidentified and reworked pollen and spores. The pollen sum excluding *Pinus* pollen regularly exceeds 170 pollen and spores (for further detail see Supplementary Material). The software Tilia was used to generate pollen diagrams and perform stratigraphically constrained cluster analysis for the delimitation of pollen zones (Grimm, 1990, 1987). Pollen accumulation rates (PARs) were calculated based on the following formula:

$$\text{PAR} = C \times \rho \times S \qquad (1)$$

with PAR in grains/(cm^2 kyr), C being the pollen concentration (grains/g dry weight), ρ the dry bulk density (g/cm^3) and S the sedimentation rate (cm/kyr). PARs have been calculated to compensate for fluctuations in the sedimentation rate that can affect pollen concentrations (Traverse, 1988). Pollen and spore taxa have been bioclimatically grouped following the modern distribution of their nearest living relatives (Table 1).

Table 1: Pollen and spore taxa from ODP *Hole* 642*B* attributed to the bioclimatic zones plotted in Figure 6.

Bioclimate groups	**Attributed pollen and spore taxa**
Cool temperate forests	*Carpinus*, *Carya*, *Corylus*, *Ilex*, *Ostrya*, *Pterocarya*, *Quercus*, *Sciadopitys*, *Taxus*, *Tsuga*, *Ulmus*
Boreal forests	*Abies*, *Alnus*, *Betula*, Cupressaceae, *Juniperus*, *Picea*
Boreal and alpine peatlands and heathlands	Asteraceae, Ericaceae, *Lycopodium* spp., *Sphagnum*

3.3. Time series analysis

In order to detect cyclicity within the vegetation changes, a continuous wavelet transform was carried out using a Morlet wavelet (Torrence and Compo, 1998). Due to the low pollen counts between 4.56 and 4.37 Ma, we only analysed the time interval from 4.37 to 3.14 Ma. For wavelet analysis, the unevenly spaced data was interpolated on 1000-year time steps prior to analysis in PAST3. In order to test whether peaks in the spectrum are significant against the red-noise background, we applied REDFIT (Schulz and Mudelsee, 2002). The analyses were performed on the relative abundance of *Pinus* pollen which dominates throughout the record.

3.4. Climate model description

Climate model output from the Hadley Centre coupled atmosphere-ocean climate model (HadCM3, Gordon et al., 2000) has been used to assess potential changes in pollen transport by wind to ODP Hole 642B in response to changes in AMOC strength, following the shoaling of the CAS. Previous studies have shown that closing the CAS is an effective means of increasing AMOC strength in a coupled atmosphere-ocean climate model (Lunt et al., 2008a, 2008b). HadCM3 has been shown to reproduce the large scale features of Pliocene climate (Haywood et al., 2013). It has been used for a number of Pliocene climate modelling studies and was the first coupled atmosphere-ocean climate model (Haywood and Valdes, 2004) to run using boundary conditions defined by the PRISM project based at the US Geological Survey.

The simulations shown here have used PRISM2 boundary conditions (following Dowsett et al., 1999). In one experiment the CAS is specified as open (hereafter referred to as OCAS) and the other the CAS is closed (hereafter referred to as CCAS; simulations are comparable to those presented in (Lunt et al., 2008b). These changes were made to assess the potential variability in AMOC strength on regional atmospheric circulation and pollen transport from

Scandinavia to ODP Hole 642B. We focus on the model output surface wind speeds and atmospheric pressure during spring (March, April, May) as most plants disperse pollen during that season.

4. Results

4.1. Pliocene pollen assemblages and vegetation reconstruction

The Pliocene pollen record of ODP Hole 642B is divided into six pollen zones (Figure 2). The complete pollen record is provided in Supplementary Material Figure 1.

Pollen Zone 1

The lowermost pollen zone (PZ 1, 83.55–77.38 mbsf, 5.03–4.51 Ma, 15 samples, two samples at the top of the zone were excluded from relative abundance calculations shown in Figure 2 due to low counts) is characterised by high abundances of *Pinus* pollen and other boreal to temperate coniferous tree and shrub taxa (*Abies*, Cupressaceae, *Juniperus* type, *Picea*, *Sciadopitys*, *Taxus* and *Tsuga*). Together with the occurrence of temperate deciduous taxa (*Carpinus*, *Carya*, *Pterocarya* and *Quercus*), PZ 1 is indicative of the presence of diverse cool temperate mixed forests in northern Norway (Figure 2). Fluctuations in the proportions of the temperate taxon *Sciadopitys* suggest that the interval was interrupted by cooler intervals that were more boreal in character. Notable are the very high pollen concentrations throughout PZ1 that decrease markedly at the top of the zone (Figure 2). The environmental interpretation of the pollen assemblages at the transition from PZ 1 to PZ 2 is hampered due to low pollen counts. The presence of mainly boreal tree and shrub taxa (*Alnus*, *Betula*, Ericaceae, *Fraxinus*, *Juniperus* type and *Pinus*) and mosses (*Huperzia* and *Sphagnum*) may be an indication of the prevalence of boreal forests and tundra environments.

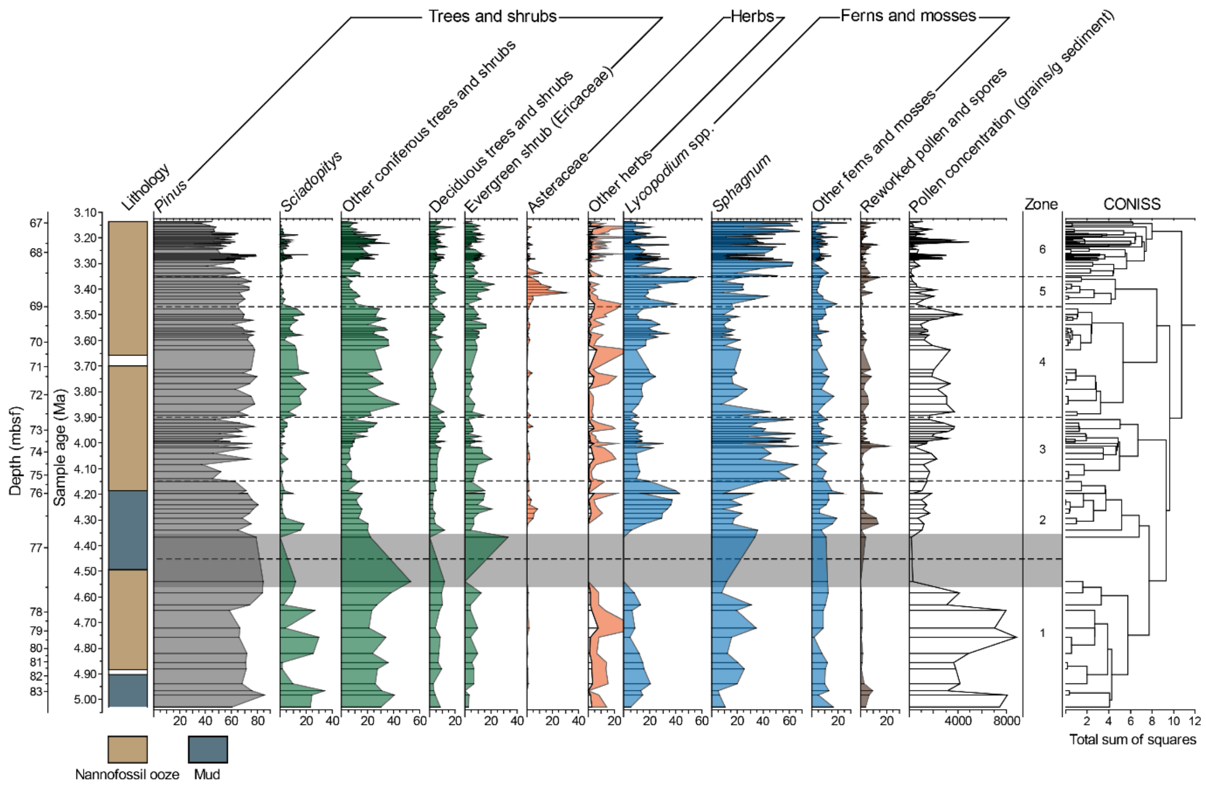

Figure 2: Abundances of pollen and spores and taxa groups in the Pliocene sediments of ODP Hole 642B. Coloured area for abundances of "other herbs" represents a 5-fold exaggeration of percentages (white area). Percentages of pollen and spores were calculated based on the pollen sum, excluding *Pinus*, unidentified and reworked pollen and spores. Only for the calculation of *Pinus* percentages were the counts of *Pinus* pollen included in the pollen sum. Depth is indicated in metres below sea floor (mbsf). Grey horizontal bar delimits samples with low pollen counts (<100). Samples with a total count of less than 40 grains are not shown. The lithology of the Pliocene section of Hole 642B was obtained from the original report (Shipboard Scientific Party, 1987).

The thermophilic but cold-tolerant taxon *Tsuga* is also present, presumably growing at favourable sites (see Supplementary Material).

Pollen Zone 2

In the middle part of pollen zone 2 (PZ 2, 76.60–75.29 mbsf, 4.30–4.15 Ma, 14 samples, two samples at the base of the zone were excluded from relative abundance calculations shown in Figure 2 due to low counts) the predominance of cool temperate forests is inferred from the relative high abundance of *Sciadopitys* pollen. The subsequent decrease in the percentages of

Sciadopitys pollen and increase in the relative proportion of Asteraceae and Ericaceae pollen as well as *Lycopodium* spores (incl. *Lycopodium annotinum*, *Lycopodium clavatum*, *Lycopodium inundatum* and *Lycopodium* spp.; Figure 2) is interpreted to reflect a southward shift of cool temperate mixed forests and an opening of the vegetation at higher altitudes due to a lowering of the treeline, leading to the development of alpine herb fields/heathlands under a boreal climate.

Pollen Zone 3

At the beginning of pollen zone 3 (PZ 3, 75.29–72.60 mbsf, 4.15–3.90 Ma, 19 samples), the relative abundance of *Pinus* pollen declines slightly whereas that of *Sphagnum* spores markedly increases. In conjunction with low proportions of other coniferous trees and shrubs taxa, these pollen assemblage changes suggest that boreal forest prevailed and peatlands expanded due to further cooling and/or wetter conditions (Figure 2).

Pollen Zone 4

In pollen zone 4 (PZ 4, 72.60–69.02 mbsf, 3.90–3.47 Ma, 25 samples), pollen of *Pinus* and other coniferous trees and shrubs predominate the assemblages, suggesting a re-establishment of cool temperate climatic conditions in northern Norway (Figure 2).

Pollen Zone 5

After this prolonged warm interval, the proportions of Asteraceae and Ericaceae pollen and *Lycopodium* spores increase in pollen zone 5 (PZ 5, 69.02–68.54 mbsf, 3.47–3.35 Ma, 9 samples, Figure 2), indicating an expansion of herb fields/heathlands at higher altitudes in response to the establishment of cooler climatic conditions and an associated lowering of the tree line. Together with the predominance of *Pinus* pollen and low abundances of other coniferous trees and shrubs, this suggests that boreal forests and alpine herb fields/heathlands prevailed in northern Norway under subarctic climatic conditions.

Pollen Zone 6

In the uppermost pollen zone (PZ 6, 68.54–66.95 mbsf, 3.35–3.14 Ma, 46 samples) the overall decline in the relative abundance of *Pinus* pollen and increasing proportion of *Sphagnum* spores is interpreted to represent the expansion of peatlands at the expanse of forests (Figure 2). Abundance peaks in the temperate taxon *Sciadopitys* point to reoccurring warmer, and thus highly variable, climatic conditions (Panitz et al., 2016). Throughout PZ 2 to 6, pollen concentrations are relatively low in comparison to those within PZ 1 (Figure 2).

4.2. Climate model results

During Northern Hemisphere (NH) spring (March, April, May), model results for both experiments indicate a predominantly westerly to southwesterly wind between 45°N and ~65–70°N (Figure 4). Between ~65–70°N and 75°N the airflow is predominantly easterly in the Nordic Seas. Whilst the dominant direction of flow south of ~65–70°N is predominantly westerly to southwesterly, over the Scandinavian land mass the details of circulation are more complex. In particular, we highlight in Figure 4 the region in central and northern Scandinavia where there is a tendency for easterly flow. The tendency for easterly flow over central and northern Scandinavia is enhanced in the OCAS scenario (Figure 4).

In the CCAS scenario, AMOC is increased relative to the OCAS scenario, with a corresponding enhancement in ocean heat transport in the NH (see Lunt et al., 2008b). This in turn alters the regional temperature and atmospheric pressure gradients over Northern Europe and the Nordic Seas (Figure 4; Lunt et al., 2008b). The result of which is to encourage stronger westerly and southwesterly flow (Figure 4), creating a corresponding suppression of easterly flow from central and northern Scandinavia into the Nordic Seas in the CCAS scenario (Figure 4). These results are most clearly expressed by surface wind and pressure patterns (Figure 4), however we have examined the nature of circulation and pressure at higher altitudes (not shown) in the atmosphere and in each case find the potential for easterly flow from Scandinavia is enhanced in the weaker AMOC scenario (OCAS).

5. Discussion

5.1. Pollen Accumulation Rates indicate changes in ocean and atmospheric circulation at c. 4.6 Ma

A distinct decline in sedimentation rate, pollen concentration and PAR at c. 4.65 Ma (Figure 2 and 3) suggests that changes in atmospheric circulation, ocean currents and/or taphonomic processes may have affected the transport, deposition and/or preservation of pollen (e.g. Dupont, 2011). The strong correlation between PARs, which takes fluctuations in sedimentation rates into account, and sedimentation rates in our record suggests potential changes in the sedimentary regime or source area. We can confidently discard any major influence of fluvial sediment transport from the Scandinavian mainland during the Pliocene. During the Oligocene to Pliocene, the inner Norwegian Sea continental shelf was the main depocentre for sediments from western Scandinavia. Hemipelagic sediments were deposited on the shelf and pelagic ooze on the slope and rise (Eidvin et al., 2014). West of the continental shelf, pelagic sedimentation (biogenic ooze) accumulated during the Oligocene to Pliocene (Eidvin et al., 2014). ODP Hole 642B is located ~450 km off the Norwegian coast at a water depth of ~1300 meter below sea level on the Vøring plateau, which was unaffected by sediment supply from Scandinavia. The Hole 642B pollen record also shows a low pollen/dinocyst (P/D) ratio (Figure 3) and a dominance of long-distance, wind-pollinated taxa (such as *Pinus*, Figure 2), both indicating a very low influence of sea level and sediment accumulation changes, if compared to Quaternary glacials and interglacials (McCarthy et al., 2003; McCarthy and Mudie, 1998). The pollen record does not show any change in the proportions of reworked pollen grains or a shift in vegetation composition at 4.65 Ma (Figure 2), indicating that preservation issues or changes in pollen production on the mainland are an unlikely cause for the decline in PAR.

At Hole 642B, stable carbon isotope values indicate an increase in bottom water ventilation between 4.65 and 4.40 Ma, reaching values closer to the Holocene mean (Risebrobakken et al., 2016). A decline in dinocyst and acritarch accumulation rates suggests a contemporaneous reduction in primary productivity (De Schepper et al., 2015), which might have affected the sinking of pollen grains to the sea floor (Dupont, 2011). These oceanographic changes broadly coincide with the deep subsidence of the Hovgård Ridge in the Fram Strait and the shoaling of CAS, with the latter resulting in an increased AMOC (Haug et al., 2001; Risebrobakken et al., 2016; Steph et al., 2010). The Neogene AMOC and its varying intensity prior to the closure of CAS during the Early Pliocene is a matter of debate. Modelling results indicate that both oceanographic circulation and associated heat transport were considerably reduced with an open CAS when compared to present-day conditions (e.g. Lunt et al., 2008b), whereas palaeobotanical evidence suggests a Pliocene steepening of the shallow thermal latitudinal gradients that existed in North America and Western Eurasia throughout the Miocene (Utescher et al., 2017). These changes might have also influenced the predominant mode of pollen transport which largely depends on the regional climate and the distance of the site from the source area (Mudie and McCarthy, 2006). Today, the main atmospheric circulation pattern in the North Atlantic region is determined by the difference in pressure between the subtropical Azores high and the subpolar Icelandic low (Furevik, 2000). During the early Zanclean, atmospheric circulation changes in the Nordic Seas region might have occurred in response to the shoaling of the CAS and its effect on the AMOC (Haug et al., 2001; Steph et al., 2010).

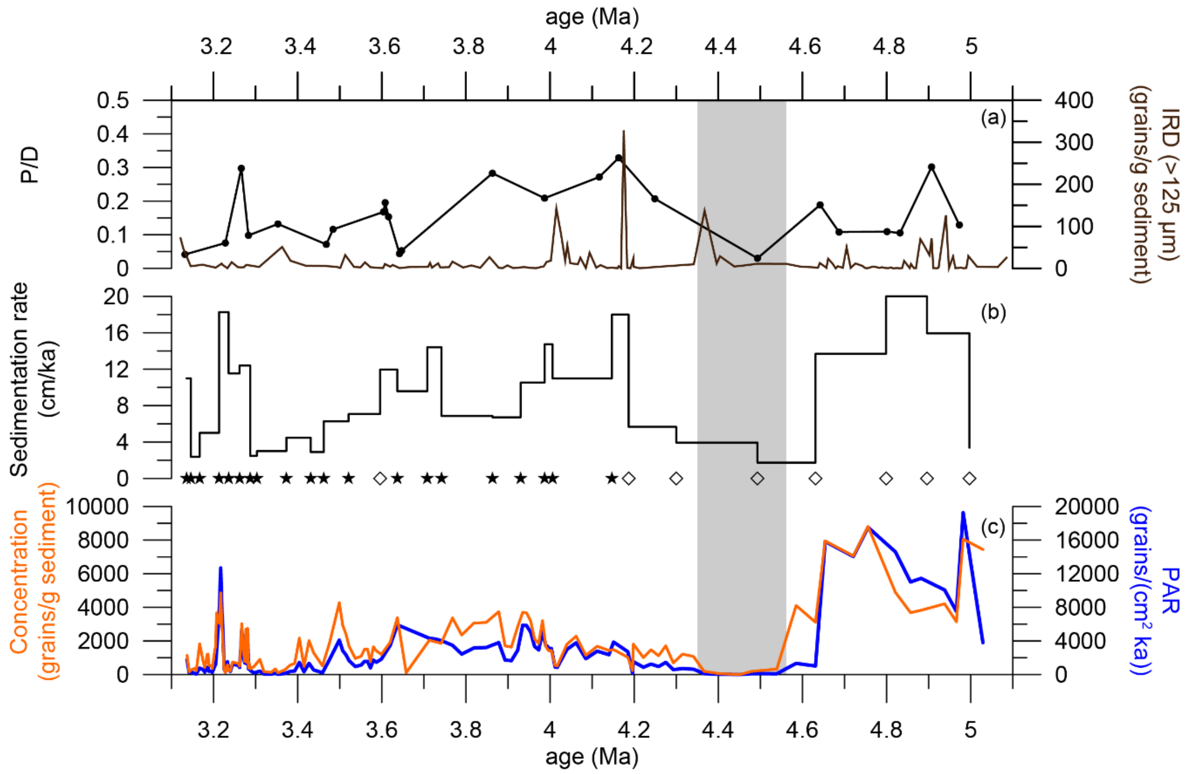

Figure 3: Sedimentological data from ODP Hole 642B. (a) pollen (P) and dinoflagellate cyst (D) ratio (De Schepper et al., 2015) and ice rafted debris (IRD) (Jansen et al., 1990); (b) sedimentation rate and age control points based on magnetic reversals (diamonds) and correlation of the benthic $\delta^{18}O$ values to the LR04 global benthic $\delta^{18}O$ stack (stars) (Risebrobakken et al., 2016); (c) pollen concentrations and pollen accumulation rates (PARs) (this study). Grey horizontal bar delimits samples with low pollen counts (<100).

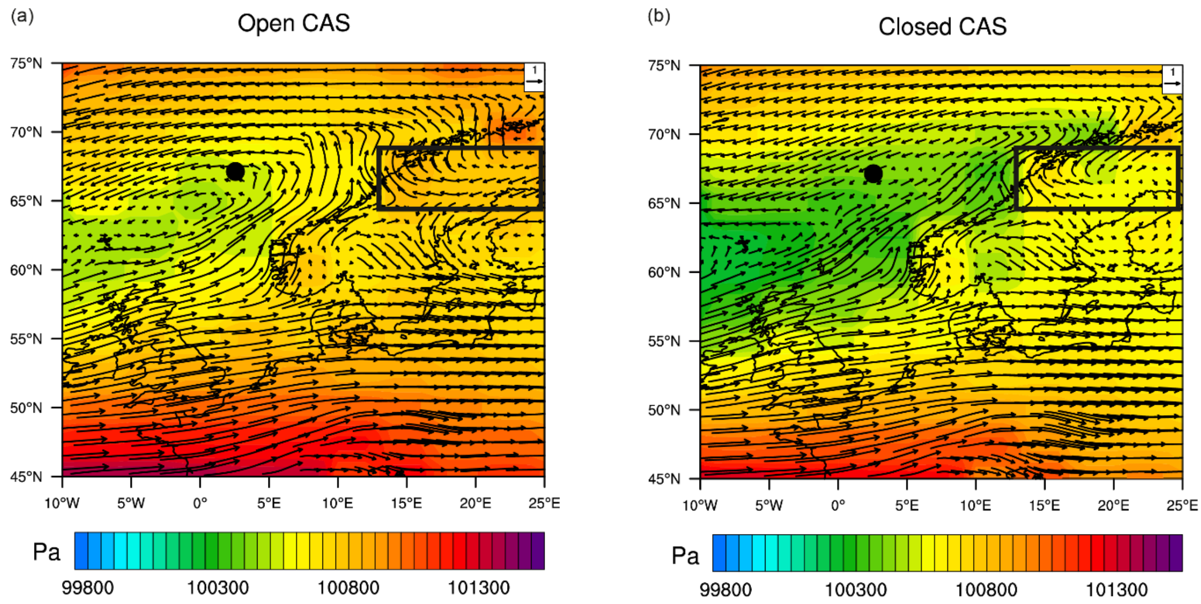

Figure 4: Model predictions for wind vectors (arrows, m s^{-1}) and mean sea level pressure (Pa) in spring (March, April, May) in the Nordic Seas region with an (a) open and (b) closed Central American Seaway (CAS). Black circle marks the location of ODP Hole 642B in the Norwegian Sea (67°N, 3°E). Black box shows an area in central/northern Scandinavia where the wind strength and direction changes significantly between the two simulations and is referred to within the main text.

To test the hypothesis of AMOC related atmospheric circulation changes affecting pollen transport to Hole 642B (potentially, but not uniquely, associated with a shoaling of the CAS), mean surface wind velocities during spring were compared from experiments with an OCAS and CCAS (Figure 4). In both experiments the predominant atmospheric flow in the Nordic Seas is westerly and south-westerly. However, the pattern of atmospheric circulation over the Scandinavian land mass is more complex. Of particular note, is the easterly flow moving out into the Nordic Seas over central and northern Scandinavia. This easterly flow is suppressed in the CCAS scenario, therefore we suggest that the potential for pollen transport from Scandinavia to Hole 642B is enhanced under weaker AMOC scenarios during the Pliocene (e.g. OCAS).

Whilst the timing of CAS closure is widely debated, our HadCM3 simulations suggest that a closing of the CAS could impact wind-fields over Norway (associated with an increase in the AMOC with a closing CAS). Therefore, this provides a potential explanation for part of the decrease in PAR after 4.65 Ma, as this lies within the uncertainty related to the timing of CAS closure (Haug et al., 2001; Steph et al., 2010). However, we also acknowledge that there are other potential mechanisms (e.g. palaeogeographic changes in the Arctic; Otto-Bliesner et al., 2017) that could cause a change in Pliocene AMOC and are not associated with the closure of CAS, which could therefore affect pollen deposition at Hole 642B.

5.2. Long-term cooling and climatic cyclicity

The Pliocene pollen record from Hole 642B reveals four major changes in vegetation and climate in northern Norway, with cooler, boreal conditions developing at 4.30 Ma and 3.47 Ma and warmer, cool temperate conditions at 3.90 Ma and 3.29 Ma (Figure 2). These changes are indicative of repeated latitudinal shifts of the northern boundary of the deciduous forest zone. Possible controls on the long-term vegetation changes in northern Norway include declining atmospheric CO_2 concentrations and astronomical forcing.

Over the almost two-million-year-long record, the relative abundance of the thermophilic taxon *Sciadopitys* shows a continuous decline during subsequent warm intervals (Figure 2). At present, *Sciadopitys* is endemic to Japan where it thrives on well-drained slopes in a temperate and wet climate (Ishikawa and Watanabe, 1986). During the Neogene, *Sciadopitys* was a common element in the temperate forests of the Northern Hemisphere, forming part of many different plant communities that inhabited diverse environments from lowland swamps to high-altitude forests (e.g. Figueiral et al., 1999). In northern Norway, the decline of this species throughout the Pliocene may be indicative of a progressive cooling of climate that is also evident in other Pliocene terrestrial and marine records (e.g. Lawrence et al., 2009; Naafs et al., 2010; Verhoeven et al., 2013). Decreasing atmospheric CO_2 concentrations have been

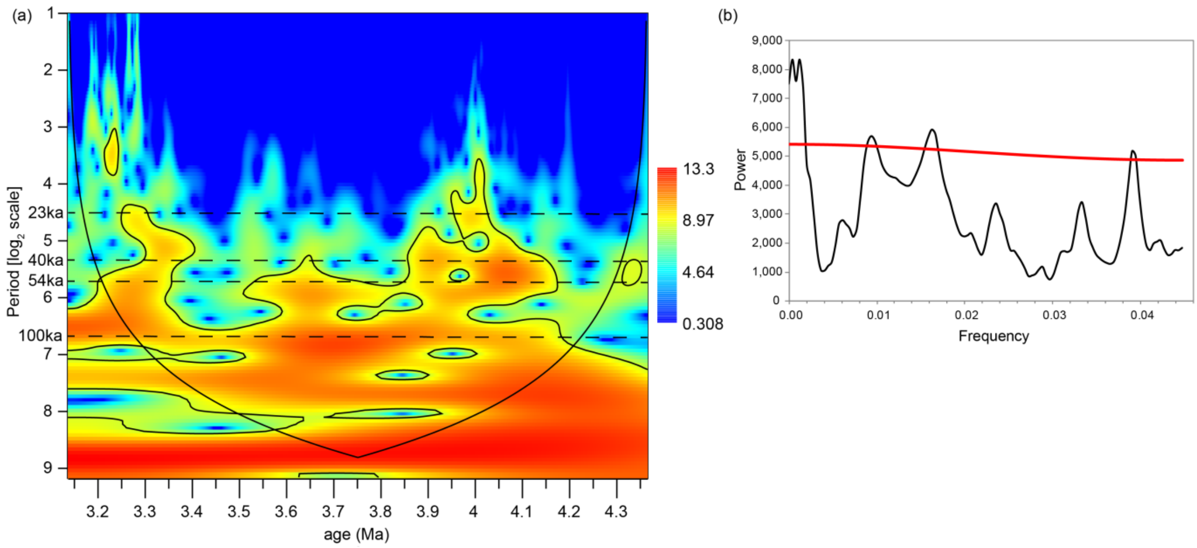

Figure 5: (a) Spectral analysis based on continuous wavelet transform of the relative abundance changes of *Pinus* pollen. Signal power is shown with a colour scale (red = higher). The black contour line indicates the significance level corresponding to p=0.05; and (b) REDFIT power spectrum (black line) testing whether peaks in the spectrum are significant against the red-noise background (Schulz and Mudelsee, 2002). False-alarm confidence level (red line) has been set to 90%.

suggested to be the main driver for the long-term cooling throughout the Pliocene leading to the onset of NHG (e.g. Lunt et al., 2008a; Martínez-Botí et al., 2015).

Continuous wavelet transform of *Pinus* pollen percentages reveals the influence of ~23-kyr precession, ~40 and 54-kyr obliquity for some intervals and relatively strong ~100-kyr eccentricity cycles (Figure 5). Low-frequency, large-amplitude changes linked to eccentricity could also be identified in the stable oxygen and carbon isotope records from Hole 642B (Risebrobakken et al., 2016). For the vegetation record, REDFIT identifies significance for the 100-kyr eccentricity, 54-kyr obliquity and the 23-kyr precession cycles (Figure 5). A dominance of precession cycles during the Pliocene has also been described from a compilation of Mediterranean SSTs and marine biomarker accumulation (Herbert et al., 2015). REDFIT could not identify significant 40-kyr obliquity cycles previously described from other marine sites in the North Atlantic for the Early and Late Pliocene (Figure 5)

(Lawrence et al., 2009; Naafs et al., 2010). However, it should be noted that the spectral and power spectrum analysis of the Hole 642B pollen record is limited due to the unevenly distributed sampling interval, which likely explains why wavelet transform could identify obliquity and precession cycles in two, relatively densely sampled intervals only. While astronomical forcing appears to be present in the Pliocene vegetation changes in northern Norway, palaeogeographic and palaeoceanographic changes during the studied time interval seem to have had a stronger influence on the long-term climate evolution of Scandinavia.

5.3. Pliocene vegetation change and North Atlantic current variability

5.3.1. Zanclean (5.3–3.6 Ma)

During the early Zanclean (5.03–4.51 Ma), cool temperate deciduous to mixed forests prevailed in northern Norway (Figure 2). Whether pure deciduous or mixed forests existed in the lowlands of the Scandinavian mountains is not clear from the pollen signal due to the low abundances of deciduous elements (see also Panitz et al., 2016). The latter is an artefact of the distance of the site from the shore which also results in the over-representation of *Pinus* pollen (e.g. Mudie and McCarthy, 2006). The presence of deciduous or mixed forests in northern Norway suggests a northward shift of the northern limit of these forest zones by 4–8° latitude, corresponding to an increase in average annual and July temperatures of at least 2–4°C and 4°C, respectively (Moen, 1999). A similar magnitude of warming is observed in alkenone-derived SST estimates from Hole 642B, with SSTs up to ~3°C higher than the Holocene average between 5.0 and 4.64 Ma (Figure 6) (Bachem et al., 2017). The alkenone-derived SSTs are likely biased towards summer temperatures as the main growth period of modern alkenone producing organisms occurs during the summer at higher altitudes due to reduced incoming solar radiation during winter (Bachem et al., 2016 and references therein). At ODP Site 982, which is situated in the path of the NAC before it enters the Norwegian

Sea, SSTs were ~6–12°C higher than present between 5.1 and 4.5 Ma (Figure 6) (Herbert et al., 2016), indicating that warmer-than-present Atlantic water entered the Nordic Seas.

At c. 4.90–4.85 Ma, 4.72 Ma and 4.63 Ma, the establishment of boreal forests and the development of peatlands at higher altitudes due to a lowering of the treeline are indicative of cooler climatic conditions in northern Norway (Figure 2). Around 4.90–4.80 Ma, glacial expansions have been inferred from ice-rafted debris (IRD) deposits in the Nordic Seas (Fronval and Jansen, 1996; Jansen and Sjøholm, 1991; St. John and Krissek, 2002). In the Norwegian Sea, IRD deposits point to the presence of sea-terminating glaciers around the Nordic Seas at 4.9 Ma (Figure 3) (Bachem et al., 2017; Jansen et al., 1990). This cooling is also recorded in alkenone-derived SST estimates from Hole 642B (Figure 6) (Bachem et al., 2017). Dinocyst assemblages from Hole 642B reveal the influence of warm temperate Atlantic water in the Norwegian Sea during the early Zanclean, but show a cooling in the warm/cold index around 4.90 Ma (Figure 6) (De Schepper et al., 2015). At the same time, enriched planktic and benthic $\delta^{18}O$ values suggest increased surface and bottom water densities due to lower water temperatures (Risebrobakken et al., 2016). The cooling is also evident in alkenone-based SSTs from ODP Site 907 in the Iceland Sea (De Schepper et al., 2015; Herbert et al., 2016). The prevalence of mixed and boreal forests in northern Norway around 4.90 Ma suggests that an extensive glaciation in Scandinavia is unlikely (Figure 2). However, variable climatic conditions in northern Norway between 5.03 and 4.51 Ma are in agreement with repeated cooling phases and related expansions of small-scale glaciations around the Nordic Seas (Fronval and Jansen, 1996).

At Hole 642B, very low PARs occur between 4.56 and 4.37 Ma (Figure 2; see section 5.1 for discussion). The pollen assemblage of the first sample above this interval is indicative of the presence of boreal forests and tundra environments in northern Norway. This interpretation should, however, be regarded with caution due to the low pollen counts. At 4.34 Ma, cool

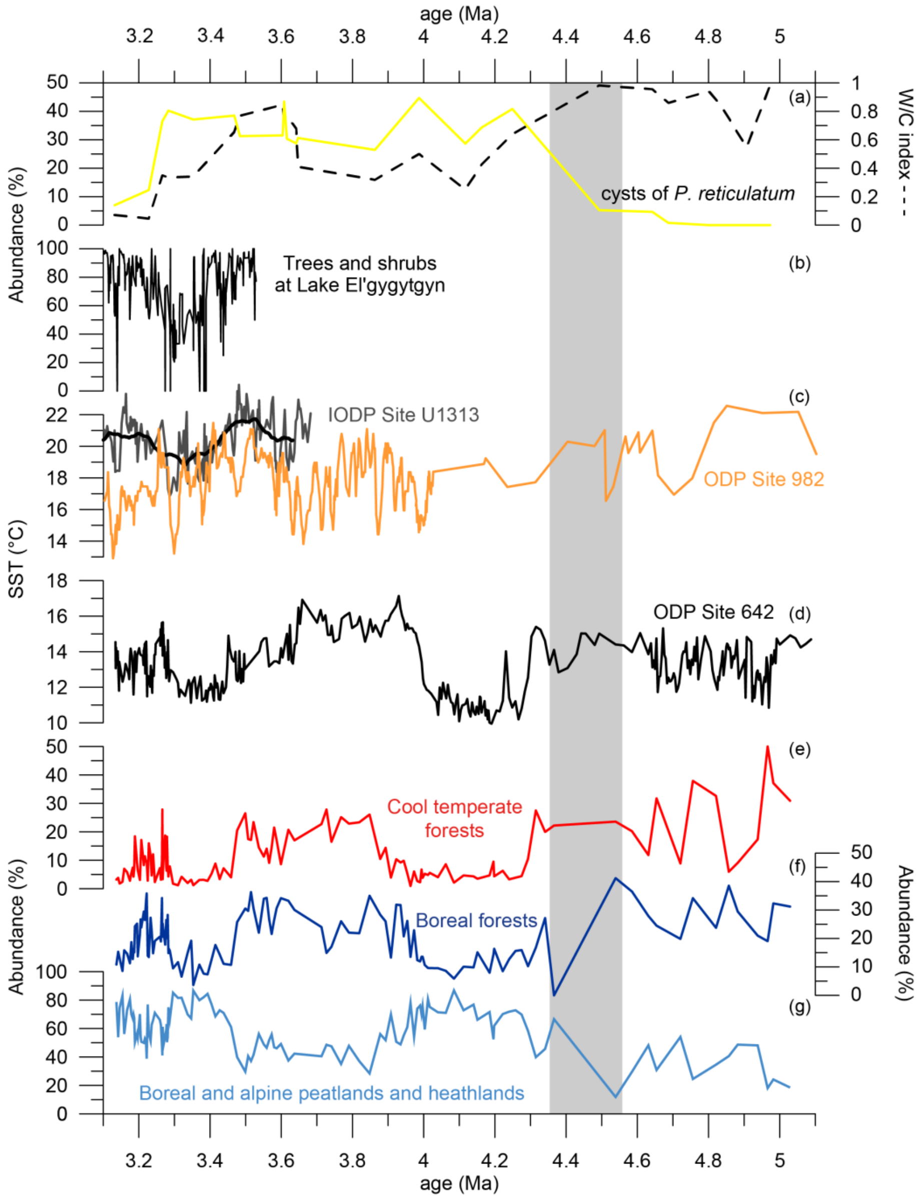

Figure 6: Comparison of predominant vegetation and climate in northern Norway during the Pliocene to other Pliocene marine and terrestrial proxy records in the Northern Hemisphere. (a) relative abundance changes of the dinocyst cyst of *Protoceratium reticulatum* (yellow) and the warm (W)/cold (C) water index (De Schepper et al., 2015); (b) relative abundance changes of trees and shrubs at Lake El'gygytgyn in NE Siberia (Andreev et al., 2014); (c) alkenone-derived sea surface temperature (SST) estimates at ODP Site 982 (orange) (Herbert et al., 2016; Lawrence et al., 2009) and IODP Site U1313 (grey) and the 100 kyr moving average (black) (Naafs et al., 2010); (d) SST estimates from ODP Hole 642B (Bachem et al., 2017); relative abundance changes of (e) cool temperate forest taxa, (f) boreal forest taxa and (g) boreal and alpine peatland and heathland taxa. For climatic grouping see Table 1. Grey bar highlights the interval with low pollen accumulation rates and counts.

temperate mixed forests indicate climate conditions similar to those before the interval with low PARs. At 4.30 Ma, the development of herb fields/heathlands at higher altitudes, followed by the expansion of peatlands at 4.15 Ma and the prevalence of boreal forests, suggests cooler climatic conditions until 3.90 Ma (Figure 2). This cooling on land coincides with the development of a modern-like NwAC between 4.50 and 4.30 Ma, as indicated by the appearance of cysts of *Protoceratium reticulatum* and an increase in cool-water dinocysts, that indicate a spread of cooler but still temperate waters across the Norwegian Sea (Figure 6) (De Schepper et al., 2015). This is supported by planktic $\delta^{18}O$ values from Hole 642B which indicate an increase in surface water salinities and/or cooling after 4.65 Ma (Risebrobakken et al., 2016). Alkenone-derived SST estimates for Hole 642B show a cooling at 4.30 Ma (Figure 6), suggesting reduced northward heat transport via the NAC (Bachem et al., 2017). At Site 982 in the North Atlantic, a slight cooling between 4.3 and 4.0 Ma coincides with reconstructed temperature changes at Hole 642B (Figure 6). However, it should be noted that the full SST variability at Site 982 is likely not recorded due to the low temporal resolution (see also Lawrence et al., 2009). At ODP Site 907 in the Iceland Sea, the gradual disappearance of dinocyst species between 4.50 and 4.30 Ma likely reflects decreasing water temperatures and salinity due to the establishment of a proto-EGC (Schreck et al., 2013). The increased export of cool Arctic waters into the Nordic Seas via a modern-like EGC has been linked to the prolonged establishment of northward water flow through the Bering Strait, possibly as a result of the shoaling of the CAS (De Schepper et al., 2015; Schreck et al., 2013; Verhoeven et al., 2011).

In northern Norway, diverse mixed forests and temperate climatic conditions re-established at 3.90 Ma (Figure 2). This warming is preceded by a rise in SSTs in the Norwegian Sea by ~6°C between 4.0 and 3.93 Ma (Figure 6) (Bachem et al., 2017) and reduced surface water densities (Risebrobakken et al., 2016), suggesting an increased inflow of warm Atlantic water as a result of an enhanced northward heat transport, following the shoaling of the CAS (Steph et al., 2010). The magnitude of warming seen in the Norwegian Sea (+ ~5°C compared to the Holocene average) is comparable to an inferred increase of July temperatures of at least 4°C in northern Norway, based on the latitudinal shift of vegetation zones (Moen, 1999). The warming in northern Norway also coincides with the emergence of seasonal sea ice in the Eurasian sector of the Arctic Ocean, with an increased sea ice export possibly counterbalancing the northward heat transport via a stronger AMOC (Knies et al., 2014). This is supported by Pliocene stable oxygen and carbon isotope records from Hole 642B, which indicate the presence of a warmer NwAC and a vigorous upper water column circulation between 4.0 and 3.65 Ma (Risebrobakken et al., 2016).

5.3.2. Piacenzian (3.6–2.6 Ma)

In northern Norway, temperate climatic conditions prevailed until 3.47 Ma (Figure 2), corresponding to SSTs up to 6°C higher than present in the Norwegian Sea and North Atlantic, indicating northward transport of warm Atlantic surface water (Figure 6) (Bachem et al., 2017; Lawrence et al., 2009; Naafs et al., 2010). At Hole 642B, a sharp decline in the relative abundance of coniferous trees and shrubs (excluding *Pinus*) between 3.48 and 3.46 Ma leads to the predominance of boreal forest and indicates a change towards subarctic climate conditions in northern Norway. This cooling coincides with a distinct decrease in alkenone-derived SST by ~2°C in the Norwegian Sea at 3.45 Ma (Figure 6) (Bachem et al., 2017). There is also indications for an increase in surface water densities in response to decreasing temperatures (Risebrobakken et al., 2016). A cooling is also recorded at Integrated Ocean Drilling Program (IODP) Site U1313 at the north-eastern edge of the subtropical gyre around 3.48–3.47 Ma (Figure 6) (Naafs et al., 2010). Following a brief warming at 3.45 Ma at Site U1313, a subsequent gradual decline in SSTs suggests a weakened NAC and northward heat transport (Naafs et al., 2010). A long-term cooling of alkenone-derived SSTs at ODP

Site 982 in the northern North Atlantic, starting at 3.5 Ma, is indicative of a gradual change of climate before the intensification of NHG (Lawrence et al., 2009). At Site 982, obliquity-driven high-amplitude SST variations during the Piacenzian are superimposed by a long-term cooling trend (Figure 6). Lawrence et al. (2009) propose that the high amplitude variations at Site 982 were caused by changes in the position of the westerlies as a result of orbitally forced insolation changes, affecting the position of the NAC.

At 3.29 Ma, corresponding to the onset of warm climatic conditions during the mid-Piacenzian (3.264–3.025 Ma), a return of cool temperate forests to northern Norway is in agreement with an increase in alkenone-derived SSTs by ~3°C in the Norwegian Sea (Figure 6) (Bachem et al., 2017; Panitz et al., 2017). A decrease in surface water densities at the site is also indicative of the presence of warmer waters in the Norwegian Sea (Risebrobakken et al., 2016). A northward shift of the NAC and accompanied re-establishment of northward heat transport is inferred from an increase in SSTs, and dinocyst assemblage changes around 3.29–3.28 Ma at several sites in the North Atlantic (De Schepper et al., 2013; Naafs et al., 2010). In the Norwegian Sea, however, the warming is not associated with changes in Atlantic water influence, suggesting that shifts in the position of the NAC are restricted to the North Atlantic. Instead, the increase in marine and terrestrial temperatures coincides with an increase in obliquity, resulting in a strengthening of the seasonal contrast (Panitz et al., 2017). In the North Atlantic and Nordic Seas region, climatic conditions seem to be slightly colder during the mid-Piacenzian than before 3.47 Ma, as seen in colder average SSTs at Site U1313 (Naafs et al., 2010), and a lower relative abundance of *Sciadopitys* pollen in the pollen assemblages of Hole 642B (Figure 6). In the Norwegian Sea, SSTs are on average only 1°C lower during the mid-Piacenzian than between 3.65 and 3.45 Ma (Figure 6) (Bachem et al., 2017, 2016). An expansion of peatlands and decline in the prevalence of boreal forests in northern Norway until 3.14 Ma are indicative of a cooling climate before the onset of NHG around 2.7 Ma (Panitz et al., 2016).

In NE Siberia, a similar pattern to the climatic changes observed at Hole 642B and Site U1313 is recorded in the relative abundance changes of trees and shrubs in the vicinity of Lake El'gygytgyn (Figure 6) (Andreev et al., 2014). While the vegetation opens around c. 3.47 Ma and c. 3.45 Ma, a pronounced decline in the relative abundance of trees and shrubs does not take place until c. 3.39 Ma. Warmer conditions establish after c. 3.28 Ma, with relative abundances of trees and shrubs accounting for >50% (Andreev et al., 2014). Changes in vegetation and climate are also recorded in northwest Africa around 3.48 Ma, with warmer and wetter conditions prevailing before and drier climatic conditions after 3.48 Ma (Leroy and Dupont, 1997). The first extensive aridification in northwest Africa at 3.26 Ma corresponds to the onset of the mid-Piacenzian, and is marked by the establishment of cool temperate conditions in Norway. The similarity between the different Northern Hemisphere records suggests that the observed climatic changes have a common forcing.

6. Conclusions

Our new high-resolution pollen record from ODP Hole 642B in the Nordic Seas enables the reconstruction of long-term climate evolution in the Norwegian Arctic during the Pliocene. The record shows multiple changes from warmer-than-present cool temperate to near-modern boreal conditions which are superimposed by a long-term cooling trend throughout the Pliocene. A comparison of vegetation changes with palaeoceanographic changes in the Nordic Sea allowed the identification of different climate forcings: shifts to a warmer-than-present Pliocene vegetation and climate with deciduous or mixed forests in northern Norway (northward shift of 4–8° latitude, average annual and July temperatures > +2–4°C and 4°C, respectively) correspond to enhanced northward heat transport via the NAC and NwAC, whereas boreal vegetation and climate occurred when northward heat transport was weaker. During the Early Pliocene, we suggest that a marked decline in PARs (c. 4.65 Ma) may have been caused by oceanographic and atmospheric circulation changes. Climate model experiments suggest that pollen transport to the site may have been reduced after c. 4.65 Ma due to changes in the atmospheric circulation pattern linked to an enhanced AMOC. An increase in AMOC might have been caused by the shoaling of the CAS between 4.8 and 4.2 Ma. A gradual decrease of relative abundances of *Sciadopitys* pollen over subsequent warm phases suggests a long-term cooling of climate, possibly in response to declining atmospheric CO_2 concentrations throughout the Pliocene. Astronomical forcing could also be identified within the vegetation record, particularly a 100-kyr cycle. However, distinct changes in vegetation and climate were linked to changes in the northward heat transport via the NAC. Our Pliocene pollen record from Hole 642B suggests that palaeogeographic and palaeoceanographic changes had a strong influence on the long-term climate evolution of Scandinavia during the Pliocene. To further understand land-sea linkages and climate forcing under warmer-than-present conditions, additional high-resolution studies along the Scandinavian coast are required, recording the spatial extent of marine and terrestrial environmental changes.

7. Acknowledgements

We would like to thank the International Ocean Drilling Program for providing the samples. We acknowledge the work of M. Jones (Palynological Laboratory Services Ltd) and Lesley Dunlop (Northumbria University) in helping with the preparation of samples. The work is part of the “Ocean Controls on high-latitude Climate sensitivity – a Pliocene case study” (OCCP) project funded by the Norwegian Research Council (project 221712). SDS also acknowledges support from the Norwegian Research Council (project 229819). AMH and

AMD acknowledge that this work was completed in receipt of funding from the European Research Council under the European Union’s Seventh Framework Programme (FP7/2007–2013)/ERC grant agreement no. 278636. We thank Paul Bachem for discussions of the results that aided data interpretation. We are grateful for comments from T. H. Donders and anonymous reviewer, which improved the manuscript.

8. Declaration of interest

Conflicts of interest: none.

9. References

Andreev, A.A., Tarasov, P.E., Wennrich, V., Raschke, E., Herzschuh, U., Nowaczyk, N.R., Brigham-Grette, J., Melles, M., 2014. Late Pliocene and Early Pleistocene vegetation history of northeastern Russian Arctic inferred from the Lake El'gygytgyn pollen record. Clim. Past 10, 1017–1039. doi:10.5194/cp-10-1017-2014

Bachem, P.E., Risebrobakken, B., De Schepper, S., McClymont, E.L., 2017. Highly variable Pliocene sea surface conditions in the Norwegian Sea. Clim. Past 13, 1153–1168. doi:10.5194/cp-13-1153-2017

Bachem, P.E., Risebrobakken, B., McClymont, E.L., 2016. Sea surface temperature variability in the Norwegian Sea during the late Pliocene linked to subpolar gyre strength and radiative forcing. Earth Planet. Sci. Lett. 446, 113–122. doi:10.1016/j.epsl.2016.04.024

Bell, D.B., Jung, S.J.A., Kroon, D., Hodell, D.A., Lourens, L.J., Raymo, M.E., 2015. Atlantic Deep-water Response to the Early Pliocene Shoaling of the Central American Seaway. Sci. Rep. 5, 12252. doi:10.1038/srep12252

Bennike, O., Abrahamsen, N., Bak, M., Israelson, C., Konradi, P., Matthiessen, J., Witkowski, A., 2002. A multi-proxy study of Pliocene sediments from Île de France, North-East Greenland. Palaeogeogr. Palaeoclimatol. Palaeoecol. 186, 1–23.

Beug, H.J., 2004. Leitfaden der Pollenbestimmung für Mitteleuropa und angrenzende Gebiete. Dr. Friedrich Pfeil, München.

Bleil, U., 1989. 40. Magnetostratigraphy of Neogene and Quaternary Sediment Series from the Norwegian Sea: Ocean Drilling Program, Leg 104. Proc. Ocean Drill. Program, Sci. Results 104, 829–901.

De Schepper, S., Groeneveld, J., Naafs, B.D.A., Van Renterghem, C., Hennissen, J., Head, M.J., Louwye, S., Fabian, K., 2013. Northern Hemisphere Glaciation during the Globally Warm Early Late Pliocene. PLoS One 8, e81508. doi:10.1371/journal.pone.0081508

De Schepper, S., Schreck, M., Beck, K., Matthiessen, J., 2015. Early Pliocene onset of modern Nordic Seas circulation due to ocean gateway changes. Nat. Commun. 6, 1–8. doi:10.1038/ncomms9659

de Vernal, A., Mudie, P.J., 1989a. Pliocene and Pleistocene palynostratigraphy at ODP Sites 646 and 647, eastern and southern Labrador Sea, in: Proceedings of the Ocean Drilling Program, Scientific Results. Ocean Drilling Program College Station, Texas, pp. 401–422.

de Vernal, A., Mudie, P.J., 1989b. Late Pliocene to Holocene palynostratigraphy at ODP Site 645, Baffin Bay, in: Proceedings of the Ocean Drilling Program, Scientific Results. pp. 387–399.

Dowsett, H.J., Barron, J.A., Poore, R.Z., Thompson, R.S., Cronin, T.M., Ishman, S.E., Willard, D.A., 1999. Middle Pliocene paleoenvironmental reconstruction: PRISM2. USGS Open File Rep.

Dowsett, H.J., Foley, K.M., Stoll, D.K., Chandler, M.A., Sohl, L.E., Bentsen, M., Otto-Bliesner, B.L., Bragg, F.J., Chan, W.-L., Contoux, C., Dolan, A.M., Haywood, A.M., Jonas, J.A., Jost, A., Kamae, Y., Lohmann, G., Lunt, D.J., Nisancioglu, K.H., Abe-Ouchi, A., Ramstein, G., Riesselman, C.R., Robinson, M.M., Rosenbloom, N.A., Salzmann, U., Stepanek, C., Strother, S.L., Ueda, H., Yan, Q., Zhang, Z., 2013. Sea Surface Temperature of the mid-Piacenzian Ocean: A Data-Model Comparison. Sci. Rep. 3, 1–8. doi:10.1038/srep02013

Dupont, L., 2011. Orbital scale vegetation change in Africa. Quat. Sci. Rev. 30, 3589–3602. doi:10.1016/j.quascirev.2011.09.019

Eidvin, T., Jansen, E., Rundberg, Y., Brekke, H., Grogan, P., 2000. The upper Cainozoic of the Norwegian continental shelf correlated with the deep sea record of the Norwegian Sea and the North Atlantic. Mar. Pet. Geol. 17, 579–600. doi:10.1016/S0264-8172(00)00008-8

Eidvin, T., Riis, F., Rasmussen, E.S., 2014. Oligocene to Lower Pliocene deposits of the Norwegian continental shelf, Norwegian Sea, Svalbard, Denmark and their relation to the uplift of Fennoscandia: A synthesis. Mar. Pet. Geol. 56, 184–221. doi:10.1016/j.marpetgeo.2014.04.006

Faegri, K., Iversen, J., 1989. Textbook of Pollen Analysis. Wiley&Sons, Chichester.

Faleide, J.I., Tsikalas, F., Breivik, A.J., Mjelde, R., Ritzmann, O., Øyvind, E., Wilson, J., Eldholm, O., 2008. Structure and evolution of the continental margin off Norway and the Barents Sea. Episodes 31, 82–91.

Feng, R., Otto-bliesner, B.L., Fletcher, T.L., Tabor, C.R., Ballantyne, A.P., Brady, E.C., 2017. Amplified Late Pliocene terrestrial warmth in northern high latitudes from greater radiative forcing and closed Arctic Ocean gateways. Earth Planet. Sci. Lett. 466, 129–138. doi:10.1016/j.epsl.2017.03.006

Figueiral, I., Mosbrugger, V., Rowe, N.P., Ashraf, A.R., Utescher, T., Jones, T.P., 1999. The miocene peat-forming vegetation of northwestern Germany: An analysis of wood remains and comparison with previous palynological interpretations. Rev. Palaeobot. Palynol. 104, 239–266. doi:10.1016/S0034-6667(98)00059-1

Fronval, T., Jansen, E., 1996. Late Neogene paleoclimates and paleoceanography in the Iceland-Norwegian Sea: evidence from the Iceland and Vøring Plateaus. Proc. Ocean Drill. Program, Sci. Results 151, 455–468.

Furevik, T., 2000. Large-scale atmospheric circulation variability and its impacts on the Nordic seas ocean climate: A review. Nord. Seas An Integr. Perspect. Geophys. Monogr. Ser. 158, 105–136.

Gordon, C., Cooper, C., Senior, C.A., Banks, H., Gregory, J.M., Johns, T.C., Mitchell, J.F.B., Wood, R.A., 2000. The simulation of SST, sea ice extents and ocean heat transports in a version of the Hadley Centre coupled model without flux adjustments. Clim. Dyn. 16, 147–168. doi:10.1007/s003820050010

Grimm, E.C., 1990. TILIA and TILIA* GRAPH. PC spreadsheet and graphics software for pollen data. INQUA, Work. Gr. Data-Handling Methods Newsl. 4, 5–7.

Grimm, E.C., 1987. CONISS: a FORTRAN 77 program for stratigraphically constrained cluster analysis by the method of incremental sum of squares. Comput. Geosci. 13, 13–35.

Groeneveld, J., Nürnberg, D., Tiedemann, R., Reichart, G.-J., Steph, S., Reuning, L., Crudeli, D., Mason, P.R.D., 2008. Foraminiferal Mg/Ca increase in the Caribbean during the Pliocene: Western Atlantic Warm Pool formation, salinity influence, or diagenetic overprint? Geochemistry, Geophys. Geosystems 9, GC1564. doi:10.1029/2006GC001564

Haug, G.H., Tiedemann, R., Zahn, R., Ravelo, A.C., 2001. Role of Panama uplift on oceanic freshwater balance. Geology 29, 207–210. doi:10.1130/0091-7613(2001)029<0207:ROPUOO>2.0.CO;2

Haywood, A.M., Hill, D.J., Dolan, A.M., Otto-Bliesner, B.L., Bragg, F., Chan, W.-L., Chandler, M.A., Contoux, C., Dowsett, H.J., Jost, A., Kamae, Y., Lohmann, G., Lunt, D.J., Abe-Ouchi, A., Pickering, S.J., Ramstein, G., Rosenbloom, N.A., Salzmann, U., Sohl, L., Stepanek, C., Ueda, H., Yan, Q., Zhang, Z., 2013. Large-scale features of Pliocene climate: results from the Pliocene Model Intercomparison Project. Clim. Past 9, 191–209. doi:10.5194/cp-9-191-2013

Haywood, A.M., Valdes, P.J., 2004. Modelling Pliocene warmth: contribution of atmosphere, oceans and cryosphere. Earth Planet. Sci. Lett. 218, 363–377.

Herbert, T.D., Lawrence, K.T., Tzanova, A., Peterson, L.C., Caballero-Gill, R., Kelly, C.S., 2016. Late Miocene global cooling and the rise of modern ecosystems. Nat. Geosci. 9, 843–849. doi:10.1038/ngeo2813

Herbert, T.D., Ng, G., Cleaveland Peterson, L., 2015. Evolution of Mediterranean sea surface temperatures 3.5–1.5 Ma: Regional and hemispheric influences. Earth Planet. Sci. Lett. 409, 307–318. doi:10.1016/j.epsl.2014.10.006

Hilgen, F.J., Lourens, L.J., Van Dam, J.A., 2012. Chapter 29 - The Neogene Period, in: The Geologic Time Scale. Elsevier, Burlington, MA, USA, pp. 923–978. doi:10.1016/B978-0-444-59425-9.00029-9

Hill, D.J., 2015. The non-analogue nature of Pliocene temperature gradients. Earth Planet. Sci. Lett. 425, 232–241. doi:10.1016/j.epsl.2015.05.044

Ishikawa, S., Watanabe, N., 1986. An ecological study on the Sciadopitys verticillata forest and other natural forests of Mt. Irazu, southern Shikoku, Japan. Mem. - Fac. Sci. Kochi Univ. Ser. D Biol. 7, 63–66.

Jansen, E., Sjøholm, J., 1991. Reconstruction of Glaciation over the Past 6 Myr from Ice-Borne Deposits in the Norwegian Sea. Lett. to Nat. 349, 600–603.

Jansen, E., Sjøholm, J., Bleil, U., Erichsen, J., 1990. Neogene and Pleistocene glaciations in the northern hemisphere and late Miocene - Pliocene global ice volume fluctuations: evidence from the Norwegian Sea, in: Geological History of the Polar Oceans: Arctic versus Antarctic. Springer Netherlands, pp. 677–705.

Knies, J., Cabedo-Sanz, P., Belt, S.T., Baranwal, S., Fietz, S., Rosell-Melé, A., 2014. The emergence of modern sea ice cover in the Arctic Ocean. Nat. Commun. 5, 5608.

doi:10.1038/ncomms6608

Lawrence, K.T., Herbert, T.D., Brown, C.M., Raymo, M.E., Haywood, A.M., 2009. High-amplitude variations in North Atlantic sea surface temperature during the early Pliocene warm period. Paleoceanography 24, PA2218. doi:10.1029/2008PA001669

Leroy, S.A.G., Dupont, L.M., 1997. Marine palynology of the ODP Site 658 (N-W Africa) and its contribution to the stratigraphy of late Pliocene. GEOBIOS 30, 351–359.

Lisiecki, L.E., Raymo, M.E., 2005. A Pliocene-Pleistocene stack of 57 globally distributed benthic $\delta18O$ records. Paleoceanography 20, PA1003.

Lunt, D.J., Foster, G.L., Haywood, A.M., Stone, E.J., 2008a. Late Pliocene Greenland glaciation controlled by a decline in atmospheric $CO2$ levels. Nature 454, 1102–1105.

Lunt, D.J., Valdes, P.J., Haywood, A., Rutt, I.C., 2008b. Closure of the Panama Seaway during the Pliocene: implications for climate and Northern Hemisphere glaciation. Clim. Dyn. 30, 1–18. doi:10.1007/s00382-007-0265-6

Martínez-Botí, M.A., Foster, G.L., Chalk, T.B., Rohling, E.J., Sexton, P.F., Lunt, D.J., Pancost, R.D., Badger, M.P.S., Schmidt, D.N., 2015. Plio-Pleistocene climate sensitivity evaluated using high-resolution $CO2$ records. Nature 518, 49–54. doi:10.1038/nature14145

McCarthy, F.M.G., Gostlin, K.E., Mudie, P.J., Hopkins, J.A., 2003. Terrestrial and Marine Palynomorphs As Sea-Level Proxies : an Example From Quaternary Sediments on the New Jersey Margin , U . S . a . Soc. Sediment. Geol. 119–129.

McCarthy, F.M.G., Mudie, P.J., 1998. Oceanic pollen transport and pollen:dinocyst ratios as markers of late Cenozoic sea level change and sediment transport. Palaeogeogr. Palaeoclimatol. Palaeoecol. 138, 187–206. doi:10.1016/S0031-0182(97)00135-1

Moen, A., 1999. National Atlas of Norway: vegetation. Norwegian Mapping Authority, Hønefoss, Norway.

Moen, A., 1987. The regional vegetation of Norway; that of central Norway in particular. Nord. Geogr. Tidsskr. 41, 179–226.

Mork, M., 1981. Circulation phenomena and frontal dynamics of the Norwegian coastal current. Philos. Trans. R. Soc. London 302, 635–647.

Mudie, P.J., McCarthy, F.M.G., 2006. Marine palynology: potentials for onshore - offshore correlation of Pleistocene - Holocene records. Trans. R. Soc. South Africa 61, 139–157.

Naafs, B.D.A., Stein, R., Hefter, J., Khélifi, N., De Schepper, S., Haug, G.H., 2010. Late Pliocene changes in the North Atlantic Current. Earth Planet. Sci. Lett. 298, 434–442. doi:10.1016/j.epsl.2010.08.023

Orvik, K.A., Niiler, P., 2002. Major pathways of Atlantic water in the northern North Atlantic and Nordic Seas toward Arctic. Geophys. Res. Lett. 29, 2-1-2–4. doi:10.1029/2002GL015002

Osborne, A.H., Newkirk, D.R., Groeneveld, J., Martin, E.E., Tiedemann, R., Frank, M., 2014. The seawater neodymium and lead isotope record of the final stages of Central

American Seaway closure. Paleoceanography 29, 715–729. doi:10.1002/2014PA002676

Otto-Bliesner, B.L., Jahn, A., Feng, R., Brady, E.C., Hu, A., Löfverström, M., 2017. Amplified North Atlantic warming in the late Pliocene by changes in Arctic gateways. Geophys. Res. Lett. 44, 957–964. doi:10.1002/2016GL071805

Panitz, S., De Schepper, S., Salzmann, U., Bachem, P.E., Risebrobakken, B., Clotten, C., Hocking, E.P., 2017. Mid-Piacenzian variability of Nordic Seas surface circulation linked to terrestrial climatic change in Norway. Paleoceanography 32, PA003166. doi:10.1002/2017PA003166

Panitz, S., Salzmann, U., Risebrobakken, B., De Schepper, S., Pound, M.J., 2016. Climate variability and long-term expansion of peatlands in Arctic Norway during the late Pliocene (ODP Site 642, Norwegian Sea). Clim. Past 12, 1043–1060. doi:10.5194/cpd-11-5755-2015

Raymo, M.E., Grant, B., Horowitz, M., Rau, G.H., 1996. Mid-Pliocene warmth: stronger greenhouse and stronger conveyor. Mar. Micropaleontol. 27, 313–326. doi:10.1016/0377-8398(95)00048-8

Raymo, M.E., Hodell, D., Jansen, E., 1992. Response of deep ocean circulation to initiation of Northern Hemisphere glaciation (3–2 Ma). Paleoceanography 7, 645–672. doi:10.1029/92pa01609

Risebrobakken, B., Andersson, C., De Schepper, S., McClymont, E.L., 2016. Low frequency Pliocene climate variability on the eastern Nordic Seas. Paleoceanography 31, 1154–1175. doi:10.1002/2015PA002918

Salzmann, U., Dolan, A.M., Haywood, A.M., Chan, W.-L., Voss, J., Hill, D.J., Abe-Ouchi, A., Otto-Bliesner, B., Bragg, F.J., Chandler, M.A., Contoux, C., Dowsett, H.J., Jost, A., Kamae, Y., Lohmann, G., Lunt, D.J., Pickering, S.J., Pound, M.J., Ramstein, G., Rosenbloom, N.A., Sohl, L., Stepanek, C., Ueda, H., Zhang, Z., 2013. Challenges in quantifying Pliocene terrestrial warming revealed by data-model discord. Nat. Clim. Chang. 3, 969–974.

Schreck, M., Meheust, M., Stein, R., Matthiessen, J., 2013. Response of marine palynomorphs to Neogene climate cooling in the Iceland Sea (ODP Hole 907A). Mar. Micropaleontol. 101, 49–67. doi:10.1016/j.marmicro.2013.03.003

Schulz, M., Mudelsee, M., 2002. REDFIT: Estimating red-noise spectra directly from unevenly spaced paleoclimatic time series. Comput. Geosci. 28, 421–426. doi:10.1016/S0098-3004(01)00044-9

Shipboard Scientific Party, 1987. 4. Site 642: Norwegian Sea, in: Eldholm, O., Thiede, J., Taylor, E. (Eds.), . Init. Repts., 104: College Station, TX (Ocean Drilling Program), pp. 53–453.

St. John, K.E.K., Krissek, L.A., 2002. The late Miocene to Pleistocene ice-rafting history of southeast Greenland. Boreas 28–35.

Steph, S., Tiedemann, R., Prange, M., Groeneveld, J., Schulz, M., Timmermann, A., Nürnberg, D., Rühlemann, C., Saukel, C., Haug, G.H., 2010. Early Pliocene increase in thermohaline overturning: A precondition for the development of the modern equatorial

Pacific cold tongue. Paleoceanography 25, 1–17. doi:10.1029/2008PA001645

Stockmarr, J., 1971. Tablets with spores used in absolute pollen analysis. Pollen et spores 13, 615–621.

Torrence, C., Compo, G. ~P. G.P., 1998. A practical guide to wavelet analysis. Bull. Am. Meteorol. Soc. 79, 61–78. doi:10.1175/1520-0477(1998)079<0061:APGTWA>2.0.CO;2

Traverse, A., 1988. Production, dispersal, and sedimentation of spores/pollen, in: Paleopalynology. UNWIN HYMAN, London, pp. 375–430.

Utescher, T., Dreist, A., Henrot, A.-J., Hickler, T., Liu, Y.-S.C., Mosbrugger, V., Portmann, F.T., Salzmann, U., 2017. Continental climate gradients in North America and Western Eurasia before and after the closure of the Central American Seaway. Earth Planet. Sci. Lett. 472, 120–130.

Verhoeven, K., Louwye, S., Eiríksson, J., 2013. Plio-Pleistocene landscape and vegetation reconstruction of the coastal area of the Tjörnes Peninsula, Northern Iceland. Boreas 42, 108–122. doi:10.1111/j.1502-3885.2012.00279.x

Verhoeven, K., Louwye, S., Eiríksson, J., De Schepper, S., 2011. A new age model for the Pliocene-Pleistocene Tjörnes section on Iceland: Its implication for the timing of North Atlantic-Pacific palaeoceanographic pathways. Palaeogeogr. Palaeoclimatol. Palaeoecol. 309, 33–52. doi:10.1016/j.palaeo.2011.04.001

Willard, D.A., 1996. Pliocene-Pleistocene pollen assemblages from the Yermak Plateau, Arctic Ocean: Sites 910 and 911. Proc. Ocean Drill. Program, Sci. Results 151, 297–305.

Willard, D.A., 1994. Palynological record from the North Atlantic region at 3 Ma: vegetational distribution during a period of global warmth. Rev. Palaeobot. Palynol. 83, 275–297. doi:10.1016/0034-6667(94)90141-4

Zhang, Z.S., Nisancioglu, K.H., Chandler, M.A., Haywood, A.M., Otto-Bliesner, B.L., Ramstein, G., Stepanek, C., Abe-Ouchi, A., Chan, W.L., Bragg, F.J., Contoux, C., Dolan, A.M., Hill, D.J., Jost, A., Kamae, Y., Lohmann, G., Lunt, D.J., Rosenbloom, N.A., Sohl, L.E., Ueda, H., 2013. Mid-Pliocene Atlantic Meridional Overturning Circulation not unlike modern. Clim. Past 9, 1495–1504. doi:10.5194/cp-9-1495-2013

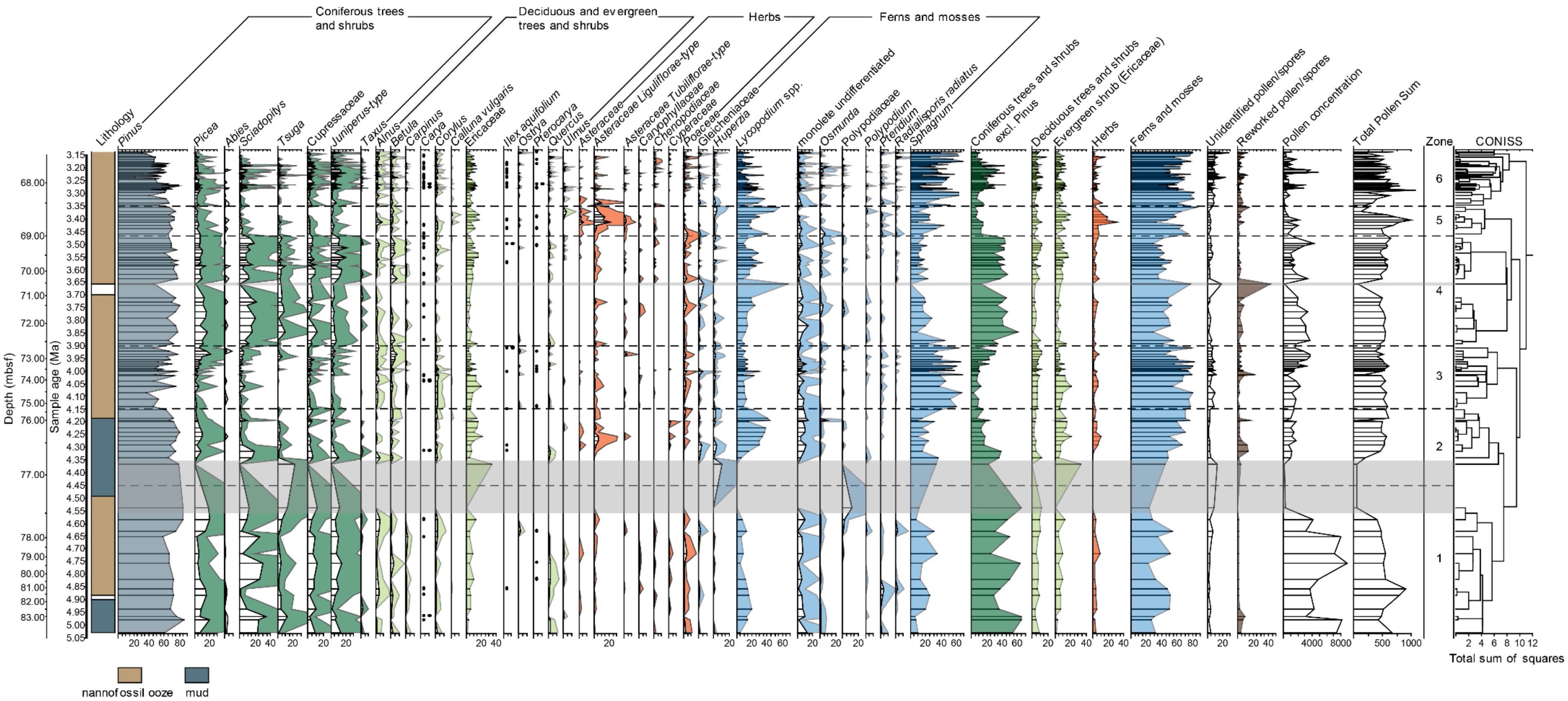

Supplementary Figure 1: Pollen assemblages in the Pliocene sediments of ODP Hole 642B. Unstriped area represents 5-fold exaggeration of percentages. Black circles are representative of single pollen or spore grains. Percentages of pollen and spores were calculated based on the pollen sum, excluding *Pinus*, unidentified and reworked pollen and spores. *Pinus* was included in the pollen sum to calculate percentages of *Pinus*. The total pollen sum shown here comprises *Pinus* and unidentified pollen. Depth is indicated in metres below sea floor (mbsf). Grey horizontal bars delimit samples with low pollen counts (<100). Samples with a total count of less than 40 grains are not shown. Colour coding illustrates the different groups of taxa. The lithology of the Pliocene section of Hole 642B was obtained from the original report (Shipboard Scientific Party, 1987).

Supplementary Table 1. Tie points used by (Risebrobakken et al., 2016) to establish the updated age model of ODP Hole 642B. The tie points are either based on magnetic reversals, updated to ATNTA2012 (Hilgen et al., 2012), or on correlating the *Cassidulina teretis* 5pt running mean $\delta^{18}O$ (Risebrobakken et al., 2016) to the LR04 global benthic $\delta^{18}O$ stack (Lisiecki and Raymo, 2005).

Chron/subchron (ATNTA2012)	Comment	LR04 Ma	ATNTA 2004/2012 Ma	642B depth interval of reversal (mbsf)	642B tie points (mbsf)	Tie points (Ma)
	KM2/KM3-top	3.136			66.95	3.136
	KM2/KM3	3.146			67.06	3.146
	KM3/KM4	3.167			67.11	3.167
	KM5/KM6	3.213			67.34	3.213
	KM6/M1	3.236			67.76	3.236
	M1/M2	3.262			68.06	3.262
	M1/M2	3.287			68.37	3.287
	M2/MG1	3.303			68.41	3.303
	MG3/MG4	3.373			68.62	3.373
	MG5	3.431			68.88	3.431
	MG5/MG6	3.462			68.97	3.462
	MG7/MG8	3.521			69.34	3.521
C2An.3n/C2r	Top Gilbert		3.596	69.87-70.11	69.87	3.596
	Gi2/Gi3	3.637			70.36	3.637
	Gi5/Gi6	3.708			71.04	3.708
	Gi7/Gi8	3.742			71.53	3.742
	Gi13/Gi14	3.863			72.36	3.863
	Gi16/Gi17	3.930			72.81	3.930
	Gi19/Gi20	3.987			73.41	3.987
	Gi20/Gi21	4.006			73.69	4.006
	Gi25/Gi26	4.147			75.24	4.147
C2Ar/C3n.1n	Top Cochiti		4.187	75.96-75.99	75.96	4.187
C3n.1n/C3n.1r	Base Cochiti		4.300	76.60-76.91	76.60	4.300
C3n.1r/C3n.2n	Top Nunivak		4.493	77.20-77.51	77.36	4.493
C3n.2n/C3n.2r	Base Nunivak		4.631	77.51-77.81	77.60	4.631
C3n.2r/C3n.3n	Top Sidufjall		4.799	79.61-79.90	79.90	4.799
C3n.3n/C3N.3r	Base Sidufjall		4.896	81.66-82.01	81.84	4.896
C3N.3r/C3n.4n	Top Thvera		4.997	83.2-83.5	83.45	4.997
C3n.4n/C3r	Base Thvera		5.235	84.11-84.4	84.255	5.235
C3R/C3An.1n			6.033	97.11-97.41	97.26	6.033